SPACE SCIENCES LABORATORY

FABRICATION AND FLIGHT EVALUATION OF LARGE-AREA ULTRASOFT X-RAY DETECTORS SUITABLE FOR SPACECRAFT APPLICATION

Final Report on NASA Contract NAS 9-11024

Principal Investigator: Dr. S. Bowyer
Project Director: Dr. M. L. Lampton

Space Sciences Laboratory Series 12 Issue 78

UNIVERSITY OF CALIFORNIA, BERKELEY

Space Sciences Laboratory
University of California
Berkeley, California 94720

Final Report

FABRICATION AND FLIGHT EVALUATION OF LARGE-AREA ULTRASOFT X-RAY DETECTORS SUITABLE FOR SPACECRAFT APPLICATION

Supported by
NASA Contract NAS 9-11024

October 1, 1971

Dr. Michael L. Lampton
Project Director

Dr. Stuart Bowyer
Principal Investigator

Space Sciences Laboratory Series 12 Issue 78

Final Report

FABRICATION AND FLIGHT EVALUATION OF LARGE-AREA ULTRASOFT X-RAY DETECTORS SUITABLE FOR SPACECRAFT APPLICATION

I. Electronics Systems Development

By a joint effort of scientific and engineering personnel at UC Berkeley, the gas proportional counter flight electronics system has been revised in five areas. These modifications of the Houston/MSC design have as their general goal the improvement of instrument efficiency, simplicity, and accuracy. A thorough description of these modifications is presented below.

A. Charge Amplifier Bandwidth Improvements

Since one of the design goals for the present research program is to determine for each X-ray event the observed charge collection time, it is of the utmost importance to achieve the greatest possible amplifier bandwidth and time resolution. In this section, theoretical and experimental investigations of cascode-FET charge amplifiers are presented. Recommendations for the actual flight hardware design are given at the end of this section.

1. Theoretical Considerations

The mesh equations for the classical cascode circuit (see Fig. 1) are:

$$g_m e_1 = -i_2 = -e_2(g_3 + sC_2 + sC_3)$$

and

$$(C_1 + C_f + C_d)\, e_1 = Q + e_{out}\, C_f \quad ,$$

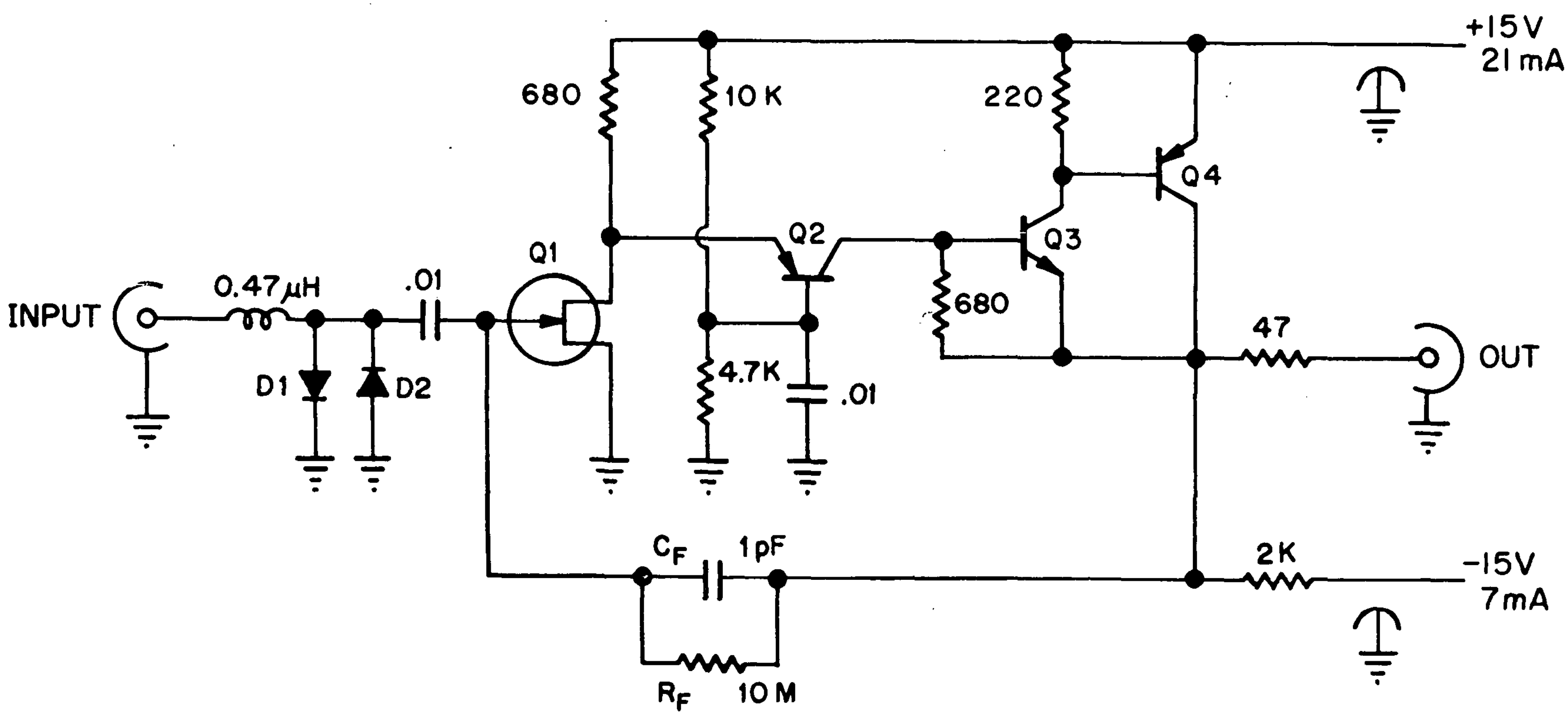

Fig. 1. Schematic diagram of the charge amplifier.
D1, D2: 1N3062 Q2, Q4: 2N5208
Q1: 2N4861 Q3: 2N4996

where $C_2 + C_3$ is the sum of the output and input capacities of the second and third transistors; g_3 is the input conductance of the third transistor (approximately $1/\beta_3 \beta_4 R_L$ mhos), and C_1, C_f, and C_d represent the capacitances for the FET gate, the feedback network, and the detector, respectively. The mutual transconductance of the FET is represented by g_m. Since $e_2 = e_{out}$,

$$\frac{e_{out}}{Q} = \frac{-\frac{1}{C_f}}{1 + \frac{g_3}{g_m} \cdot \frac{C_1 + C_f}{C_f} + s\,\frac{(C_1 + C_f + C_d)(C_2 + C_3)}{g_m C_f}}$$

This equation expresses the loop response to charge as a function of frequency ($s = i\omega$). Its nominal gain, $-1/C_f$, is diminished somewhat at all frequencies by the second term in the denominator, and is diminished at high frequencies by the third denominator term. A measure of the loop risetime is the time τ required for the output error to decay by a factor of 1/e when the input is a step function. For a first-order equation, this time constant is exactly the reciprocal of the "3 db frequency" at which the real and imaginary parts of the denominator are equal:

$$\tau = \frac{(C_1 + C_f + C_d)(C_2 + C_3)}{g_m C_f + g_3(C_1 + C_f + C_d)} \cong \frac{C_1 + C_f + C_d}{C_f} \cdot \frac{C_2 + C_3}{g_m} .$$

The approximate form is valid when the loop gain is near its nominal value. The first factor in this approximate form contains the detector and feedback capacities and measures the closed loop voltage gain required of the detector/amplifier system. The second factor contains those quantities under direct control of the engineer and represents the consequence of the finite gain-bandwidth product of the amplifier, $g_m / 2\pi(C_2 + C_3)$. Radio-frequency transistors having collector capacitances less than 1 pF are available, and low noise FETs with g_m >10 mmho have been available for many years. Consequently, gain bandwidth products in excess of 1000 MHz are easily obtained. The circuit shown in Figure 1 provides a gain bandwidth product of this order, as evidenced by the measured rise-time data given in Figure 2.

2. Experimental Considerations.

Tests on the basic circuit of Figure 1 were carried out in September 1971. This design was found to perform close to the theoretical predictions outlined above and showed a gain-bandwidth product in excess of 1000 MHz. Its noise performance was measured with an Ortec 419 precision pulse generator, an Ortec 485 main amplifier, and a Northern Scientific NS-605 pulse height analyzer. The measured root-mean-square charge noise was 740 electrons rms at a total input capacity $C_1 + C_f + C_d = 90$ pF, again in close agreement with the theoretical noise prediction. Gain stability was found to be excellent. With $C_f = 1$ pF, a detector capacitance change of 50 pF produced a closed-loop gain change of only 0.6%. Power supply variations of ±1 volt gave a gain change of less than ±0.2%. It is recommended that the basic circuit be provided with a series radio-frequency rejection trap (shown) which is self-resonant at the carrier frequency of the rocket PCM-FM transmitter. This trap was found not to affect the excellent loop risetime, and should provide 30 to 40 db improvement in rejection of radio-frequency interference.

The present design has no need for critical charge-compensation positive feedback adjustments and provides a factor of 2.5 improvement

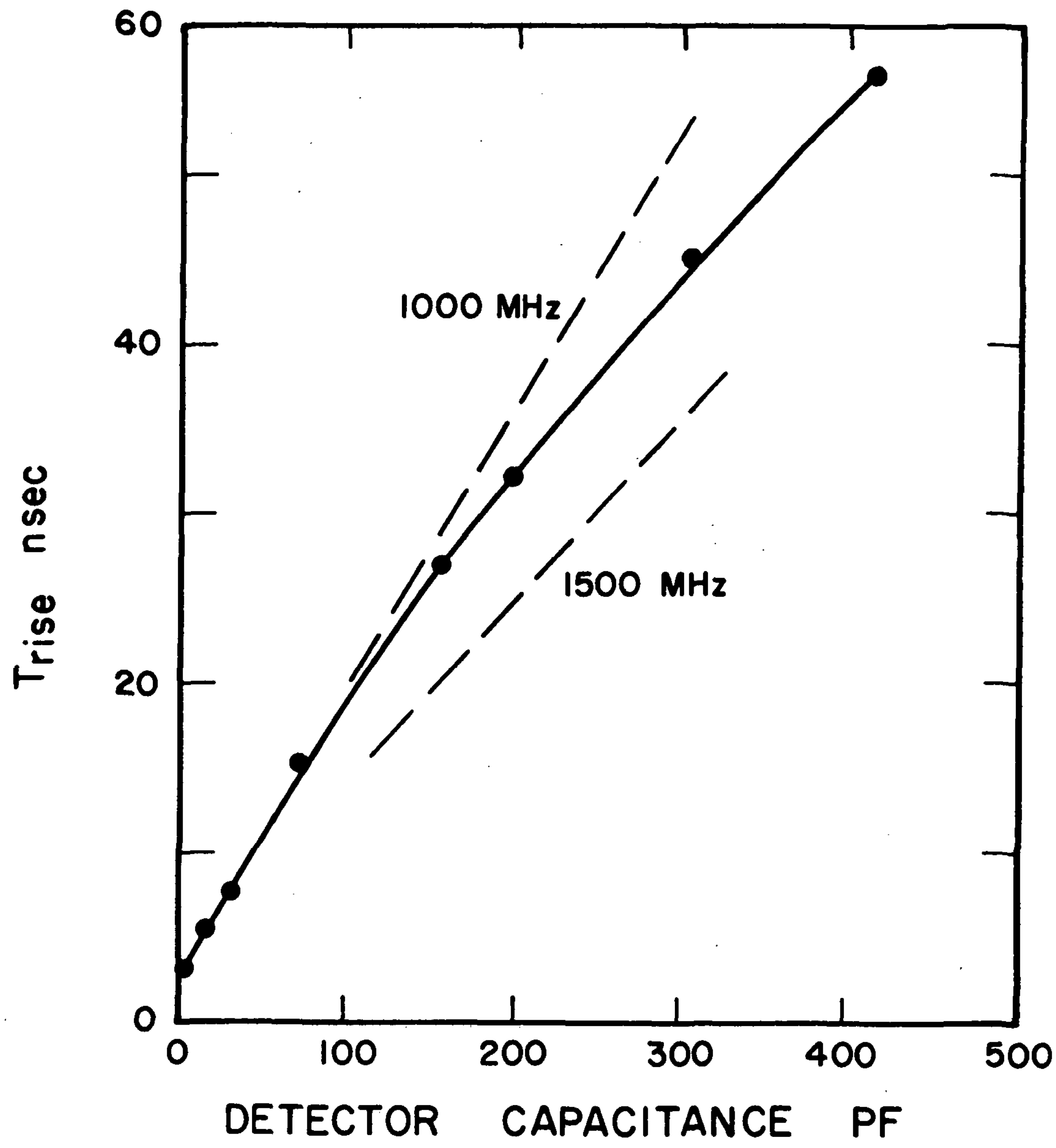

Fig. 2. Solid curve: measured risetime to 1/e when C_F = 1 pF. Dashed lines: theoretical performance for GBW = 1000 MHz and 1500 MHz.

in bandwidth over the earlier Houston/MSC design. In addition, it requires only four transistors rather than seven, uses about one-half the electrical current, and requires no heavy, unreliable high-inductance filter chokes.

B. Power Converter Redesign

Electrical power for sounding rocket instrumentation is routinely available from the primary battery pack at +28 volts. The gas proportional counter electronics requires the following electrical power buses:

+28 vdc	40 mA for HV power converter
+15 vdc	195 mA for amplifiers and PHA
+5 vdc	460 mA for logic IC's
-15 vdc	180 mA for amplifiers and PHA

To eliminate interdependence between instruments with respect to secondary power supply, it is desirable to provide +15, +5, and -15 volt power from the inboard power converter. This has been accomplished by designing a regulated power dc-dc converter having these three outputs, rather than the two provided by the original Houston/MSC design.

The new design is shown in Figure 3. Here, a series regulator in the input circuit accepts battery power at any voltage between +25 and +40 vdc, and delivers regulated +23 vdc to the square-wave dc-ac converter. This input regulator is based on the proven μA723 integrated circuit regulator/reference supply. Separate secondary windings on the saturating core square-wave transformer permit the desired output voltages to be tapped off at high efficiency. Conversion back to dc is performed by conventional full-wave rectification and filtering. Desirable features of this new design are: Complete protection against reversed polarity

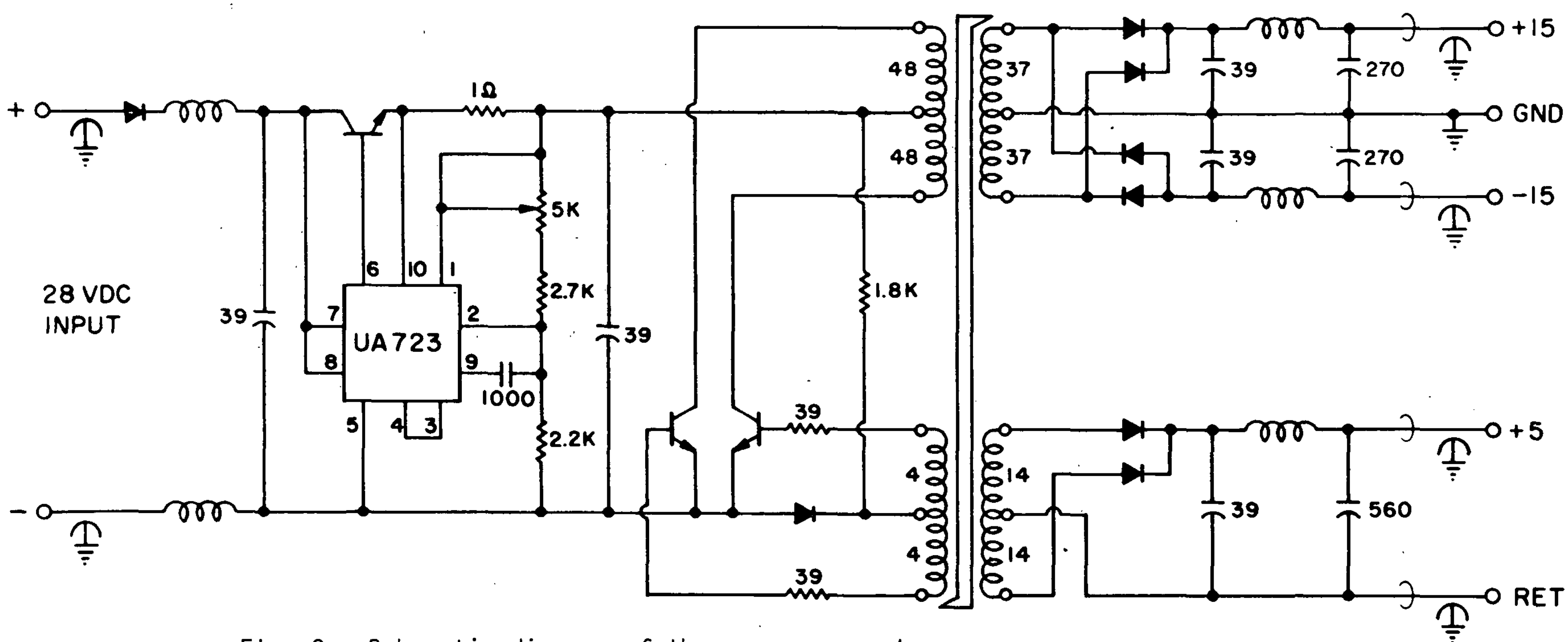

Fig. 3. Schematic diagram of the power converter.

Transistors	:	2N5191
Diodes	:	1N5061 or Varo VE18X
Capacitors	:	Sprague 145D tantalum
Inductors	:	40t on Magnetics Inc 55048-A2 ferrite core 125 perm
Transformer core	:	Magnetics Inc 52033-1D permalloy 1-mil tape
RFI terminals	:	USCC type 1021-000.

battery power; thorough input filtering against power line noise pickup and generation; short-circuit protection; and separate primary power return to avoid dc ground loops. The measured characteristics of this power converter are listed below.

Power Converter Data

Required input:	+25 to +40 vdc, 440 mA loaded
Outputs:	+15 vdc at up to 250 mA
	+5 vdc at up to 500 mA
	-15 vdc at up to 250 mA
Efficiency:	64% at +28 vdc input
Output ripple:	2 mV pp on either +15 or -15 V lines
	5 mV pp at +5 vdc line
Input ripple:	9 mA pp on battery line
Regulation:	±2% on ±15 vdc, half to full load
	±1% on ±15 vdc, input 26 to 36 vdc
Short circuit input current:	660 mA

C. Serial Data Output Buffer

In order to interface the gas proportional counter electronics system with existing sounding rocket PCM-FM telemetry systems, we have redesigned the output circuits to provide the necessary serial data flow. In such a format, the individual bits are transferred to the experiment data bus in a fixed sequence each time an interrogate signal is generated by the PCM encoder. The principal advantage of such a system is its compatibility with the Goddard Space Flight Center PCM encoder (and with the UCB, Phoenix

Data, and Monitor Systems encoders). An additional advantage is the substantial reduction in the amount of wiring required in the rocket payload section; one data wire per experiment, rather than eight, is needed.

This design was implemented with standard and low-power TTL digital integrated circuits. An eight- or nine-bit shift register is clocked by the PCM bit synchronization signal whenever a word interrogate command is received. The shift register is loaded when it is not being read out, and when an unread X-ray event has been presented for transmission.

D. Second Differentiator

The output signal from a gas proportional counter consists of a fast component arising from electron motion, and a slow component arising from ion motion. The usual shaping amplifiers provide a single-differentiated pulse, in which low-frequency components of the waveform have been substantially attenuated. The transfer function of such a shaper is given by

$$F(\omega) = \frac{i\omega t}{1 + i\omega t} \cdot \frac{1}{1 + i\omega t + (i\omega t)^2/2} ,$$

whose poles lie at i/t, $(i - 1)/t$, and $(i + 1)/t$. Such a response is characteristic of the pseudo-gaussian shaper having a time constant t.

We have modified the existing shaping network to provide a substantial improvement in the baseline stability against perturbations by the low rate-of-change ion collection currents. A second differentiator having a response function $i\omega t/(1 + i\omega t)$ has been introduced into the amplifier chain, causing low-frequency components to be attenuated by an additional factor of ωt.

E. Risetime Discriminator

The existing Houston/MSC risetime discriminator (based on the design of L. L. Lewyn, *Nuclear Instrumentation & Methods* **82**, 138, 1970) has been replaced with a version of the risetime-to-pulse-width converter described by Kinbara and Kumahara (*Nuclear Instrumentation & Methods* **70**, 173, 1969). This revision removes the requirement for a long-delay wideband lumped constant delay line, and permits measurements of risetimes to be carried out, rather than simple yes-no discriminations. Such measurements are useful not only in laboratory investigations of proportional counter behavior, but also, with further development, may prove valuable as telemetered data associated with main detector events.

The basic circuit is shown in Figure 4. Here, the unshaped delayed pulse is compared with attenuated, undelayed replicas of the pulse under study. The comparisons are performed by integrated circuit comparators, one of which trips when the signal reaches 10 percent of its final value and the other at the 90 percent point. The time interval between these trip points is just the risetime of the signal pulse between its 10 percent and 90 percent points. The delay line need not provide a delay longer than the slowest rising acceptable pulse, and the result of the measurement is available for telemetry after this minimum interval. No risetime amplifiers are required.

For use as a one-bit (yes-no) discriminator, a timing circuit is started at the 10 percent point and clocks a data storage flipflop at the end of its fixed timing interval. The datum thus recorded is the state of the other (90%) comparator at that instant.

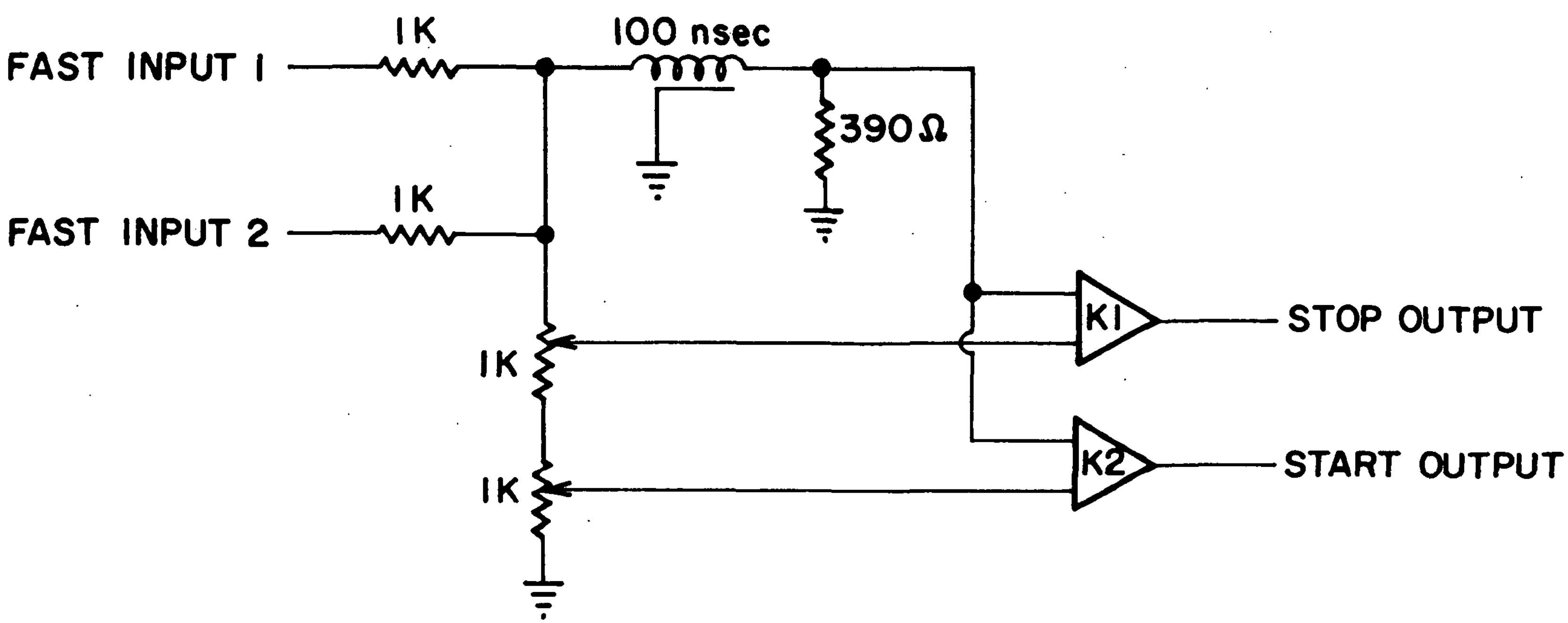

Fig. 4. Schematic diagram of the risetime discriminator.

II. Stellar Aspect Camera

Optical, mechanical, and electronic redesign of the Houston/MSC stellar aspect camera has been completed. The new design is intended to be used with any 250-exposure 35-mm camera, and requires no mechanical or optical modifications of the camera body or film magazine. Salient features of the new design are listed below.

A. Optical

The essential requirement of the optical layout is to have fiducial marks and the exposure sequence number recorded on the film simultaneously with the star field exposure being taken. In the new design, this is accomplished from outside the camera by means of two peripheral field fiducial assemblies. Each assembly contains six gallium arsenide light-emitting diodes (LED's), mounted on a small circuit board at the focal plane of a 10-mm diameter, 22-mm focal length achromatic lens. This lens directs a parallel pencil of rays from each LED toward the camera lens, which then focuses this pencil onto the film plane as an image of the LED. The desirable feature of this method is that, even though the camera lens might be put out of alignment with the payload during launch, the fiducial images are recorded through the lens in the same way as star images are, and proper aspect information will be recovered. In brief, the camera is required to record only the differences of angle correctly, and not the angles themselves; thus camera misalignment does not affect the aspect derivation. To obtain the exposure sequence number, four of the six LED's in each fiducial assembly are keyed on and off in a binary code representing the sequence number. This binary number is also transmitted simultaneously with the exposure via the PCM telemetry link; thus the time of the exposure becomes part of the flight record.

B. Mechanical

As opposed to the extensive machining required for the Houston/MSC design, no mechanical modifications of the Nikon F camera body or its electric-drive 250-exposure magazine are required. Thus, existing GSFC cameras and spares may be employed.

C. Electronics

An extremely simple camera control/fiducial generator electronics support system has been designed. The basic timing circuit is a simple low-frequency oscillator which provides an adequate frequency stability of about 1 percent against the expected variations in temperature and primary battery voltage. No power is borrowed from other rocket subsystems, since the control box includes its own dc-dc power converter. Both the film advance pulse and the shutter control pulse are derived from simple monostable timing circuits (type SN74121N) from the basic oscillator. Each shutter pulse also is applied to an exposure counter (an eight-bit ripple counter comprising two SN7493N integrated circuits). The contents of this counter are telemetered at the basic subframe rate of the PCM system, and change only when a new exposure has begun. The contents of this counter are also displayed continuously by the LED's in the fiducial assemblies.

This design, which is substantially simpler than the original one, permits substantially greater flexibility in that all timing functions can be set for any desired exposure rate and interval. Power consumption has been substantially reduced as well.

III. Thin Film Development

The fabrication of thin films was thoroughly investigated. Thin films of a variety of polymer materials were prepared by allowing a solution of the resin to spread on a water surface. It was found that the necessary condition for spreading is for the surface tension of the solution to be less than that of the aqueous substrate. If this condition is satisfied, a drop of solution placed on a water surface extends into a thin layer. If the vapor pressure of the solvent is in a suitable range, this layer dries immediately upon formation, resulting in the production of a continuous solid film.

Excessively rapid drying may interfere with the spreading process, yielding ragged films having a characteristically shredded appearance. An example of this is provided by films made from a solution of VYNS resin in ethylene dichloride. On the other hand, slow-drying results in the formation of initially liquid films which become markedly inhomogeneous as they dry and which are prone to pinhole formation. This occurs consistently in VYNS films made from an isophorone solution.

A. Recipes

1. VYNS

A solution of 1 part VYNS resin in 9 parts cyclohexanone by weight has been found to be satisfactory. More dilute solutions tend to yield films which are too thin (less than 5 micrograms per cm^2) to be handled in reasonably large sections, whereas films obtained using more concentrated solutions exhibit nonuniformity and streaking associated with excessively rapid drying. The degree to which these characteristics are present, however, depends upon both the dexterity of the film-maker and the details of the technique used.

2. Formvar 15/95

This resin dissolves in fewer of the common solvents than does VYNS. Ethylene dichloride alone is unsuitable because of its high vapor pressure and, consequently, fast drying rate. Drying may, however, be retarded by using cyclohexanone as a diluent in the ratio 1 part ethylene dichloride to 1.4 parts cyclohexanone by weight. Although not a solvent for Formvar 15/95, cyclohexanone is evidently not a precipitant and causes no problems as do some additives.

A solution of 1 part Formvar in 12 parts of the above mixture by weight is considerably more viscous than the optimum VYNS solution but yields films of good quality. More dilute solutions might be preferable but experience indicates that the proportion of cyclohexanone to ethylene dichloride should not be increased.

B. Preparation of Solutions

The polymer resins dissolve slowly and tend to clump together into sticky masses which, once they are formed, may be dispersed only by heroic efforts. This problem may largely be avoided by adding the powdered resin a little at a time to the full measure of solvent, stirring rapidly all the while.

Commercial polymer resins typically possess a considerable spread in molecular weights. Since fractions with differing molecular weights dissolve at differing rates, a freshly prepared solution should be vigorously agitated from time to time for a period of several days before use in order to ensure that true solution and equilibrium viscosity have been achieved. Otherwise, the usual problem of film nonuniformity will arise.

C. Film Production

Basically, films are made by dipping a straight-edged blade coated with a resin solution into a pan of water. Since the film dries as it forms, it spreads in one direction only, forming a long strip whose width is approximately the same as that of the blade. The following details of procedure should be followed if consistently good films are to be obtained.

1) A shallow pan of water should be used. This effectively tends to damp out water waves and so minimizes the effects of building vibrations and other disturbances.

2) The blade should be coated with resin solution as uniformly as is possible. In practice, a small quantity of solution deposited on one end and allowed to run down its length coats the blade with sufficient uniformity for most purposes.

   Although immersion of the blade in a vat of solution might in principle be preferable, improved uniformity would not be realized unless steps were taken to ensure uniform draining of excess solution from the blade after removal from the vat.

3) The blade should make contact with the water at a flat angle (less than 20 degrees). If the dip angle is steep, the resin solution flows off the blade at varying rates which are influenced by the local nature of the blade surface, and nonuniform (streaky) films often result. At flat angles, such rheological difficulties do not arise, but since a fair portion of the back of the blade contacts the water, greater surface disturbance and wave generation occur. If care is taken to ensure that the solution does

not coat the edge of the blade, careful dipping allows back contact to be made first, as shown in the accompanying diagram.

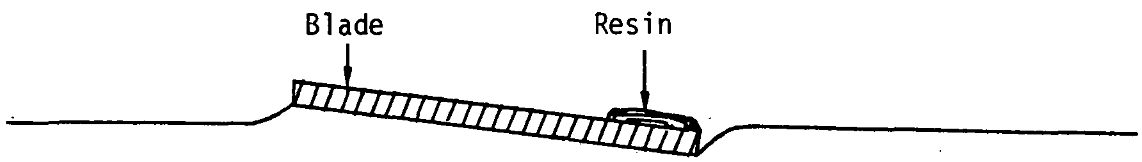

After any disturbance has died down, spreading may be initiated by a slight dipping motion of the blade edge.

A suitable frame is lowered carefully onto the film and allowed to touch the bottom of the pan. Excess film is gathered up and tucked around the edges of the frame. The film is then removed by slowly raising one edge of the frame while keeping the opposite one fixed until the frame stands vertically in the water at which time it may be lifted clear.

The tendency of large VYNS films to tear upon removal may be reduced by squirting ethanol around the edges of the frame just before lifting. Ethanol attacks Formvar 15/95 and is thus not suitable for use with this material. However, since most substances substantially reduce the surface tension of water, it should not be difficult to find an appropriate substitute.

VYNS films are hydrophobic and generally may be picked up without adhesion of water droplets. This is not the case with Formvar, which must be washed. For this purpose, a squeeze bottle of distilled water is satisfactory if the stream from the bottle strikes the film at a small angle.

VYNS requires no further preparation, but Formvar being extremely hygroscopic must be dried. Baking for 1 to 2 hours at 150 °F appears to be adequate. WARNING!!! Wet Formvar is very fragile and must be handled with extreme care prior to oven-drying.

D. Lamination

Several thin films may be superposed to produce a thicker one by the following technique.

Two films mounted on frames are placed face to face, their planes intersecting at a small angle. For this purpose it is necessary that one of the frames be slightly larger than the other. The frames are brought into contact along one edge and the angle between them is slowly reduced until contact is made around the entire perimeter of the frames.

When placed in close proximity, the vibrations of the two films become strongly coupled in-phase, and lamination might not occur. If not, it may be induced by forcing the films gently into contact near one edge by blowing upon them.

The film may be cut away from one of the frames with a hot soldering iron leaving two superposed films attached to the remaining frame.

Up to three layers may be superposed successively in this manner. Thereafter, the masses of the two films to be laminated are sufficiently different to prevent in-phase coupling of their vibrations. Contact may then occur simultaneously at many points with consequent wrinkling and entrapment of air bubbles.

E. Transfer and Mounting

Transfer of films to mesh supports is a straightforward and simple procedure provided that the latter are flat and wrinkle-free. To ensure this, the mesh should itself be bonded to a suitable frame with epoxy or some other rigid (non-elastomeric) adhesive. While the adhesive is drying, the mesh should be pulled taut with just enough tension to eliminate wrinkles and sagging. It is not advisable to oven-cure the cement since, upon cooling, differential contraction of the mesh and its frame may cause the mesh to tear.

The frame holding the film, which must be larger than the frame on which the mesh is mounted, is then carefully lowered just enough so that the film makes good contact with the mesh. At contact, the film and mesh should be parallel. The film may then be cut away from its mounting frame with a hot soldering iron.

In general, VYNS adheres well enough so that it need not be cemented to the mesh, but it is advisable to tack down Formvar (and Parylene) films around their edges. For this purpose, epoxy adhesives are preferable since they generally contain no solvents capable of attacking the films.

F. Miscellaneous

Resin solutions should be stored in tightly capped containers in order to prevent evaporation of the solvent and consequent changes in concentration. Since this will inevitably result from repeated opening, it is advisable to make up solutions in small batches (100 cc).

VYNS resin is obtainable from:	Union Carbide Corporation 2770 Leonis Boulevard Los Angeles, California 90058
Formvar 15/95 is supplied by:	Monsanto Company 6670 E. Flotilla Street Los Angeles, California 90022.

IV. Strength of Thin Films

It is not possible to give a simple general definition of the strength of a polymer. These substances are visco-elastic rather than elastic and as such have

a) grossly nonlinear stress-strain curves, and

b) apparent tensile moduli which, at a given stress level, decrease with time.

From the point of view of counter window design, it is important to know what size mesh is necessary to support a film of given thickness under a given pressure load. In the light of the foregoing discussion, it is clear that a complete answer cannot be given without specification of

a) the lifetime of the window, and

b) its maximum permissible deformation during that time.

Since tensile modulus and strength are dependent not only upon the length but also on the degree of entanglement of the polymer chains, it is moreover to be expected that properties of the bulk materials will not be accurately reflected in the behavior of thin polymer films.

Ignoring time-dependent properties, a useful if incomplete measure of the strength of a mesh-mounted thin film is its burst pressure, i.e., the differential pressure load which must be applied across the film to cause rupture. Burst pressure is proportional to tensile stress at failure or tensile strength.

A. Conditions of Measurement

Film samples to be tested were mounted on 3/16-inch i.d. annular test rings, which served to separate a small vacuum chamber from a large bell jar. One face of each ring was covered with standard nickel electroformed mesh, which was attached with Eastman 910. The mesh was held taut while the adhesive dried in order to offset a tendency of the mesh to wrinkle and crease. The film samples adhered well enough to the mesh that it was not necessary to tack them down.

After evacuation of both the bell jar and the small chamber, air was admitted to the latter through a needle valve causing the pressure differential across the film to build at a rate of approximately 200 mm Hg per minute. Film rupture was marked by an abrupt decrease in pressure.

Extensive tests using several mesh sizes and film thicknesses were conducted for VYNS in order to establish the relationship of burst pressure to these quantities. Parameters of the relationship were then obtained for samples of Formvar 15/95, Parylene N, and Parylene C. Film thicknesses were in all cases determined by weighing samples taken from the same sheet of film. All measurements were conducted at room temperature (20 °C).

B. Results

In Figure 5, the burst pressure P is plotted versus the reciprocal of the space between mesh wires, S, for several values of film thickness, t. The data, obtained for VYNS, strongly suggest a relationship of the form

$$P = k\ t\ S^{-1} .$$

Values of the constant k for the materials tested are tabulated below. The errors reflect the uniformity of the samples tested.

Material	k, mm Hg-in/μg/cm^2
Formvar	0.44 ± 0.01
Parylene C	0.33 ± 0.01
Parylene N	0.32 ± 0.01
VYNS	0.22 ± 0.03

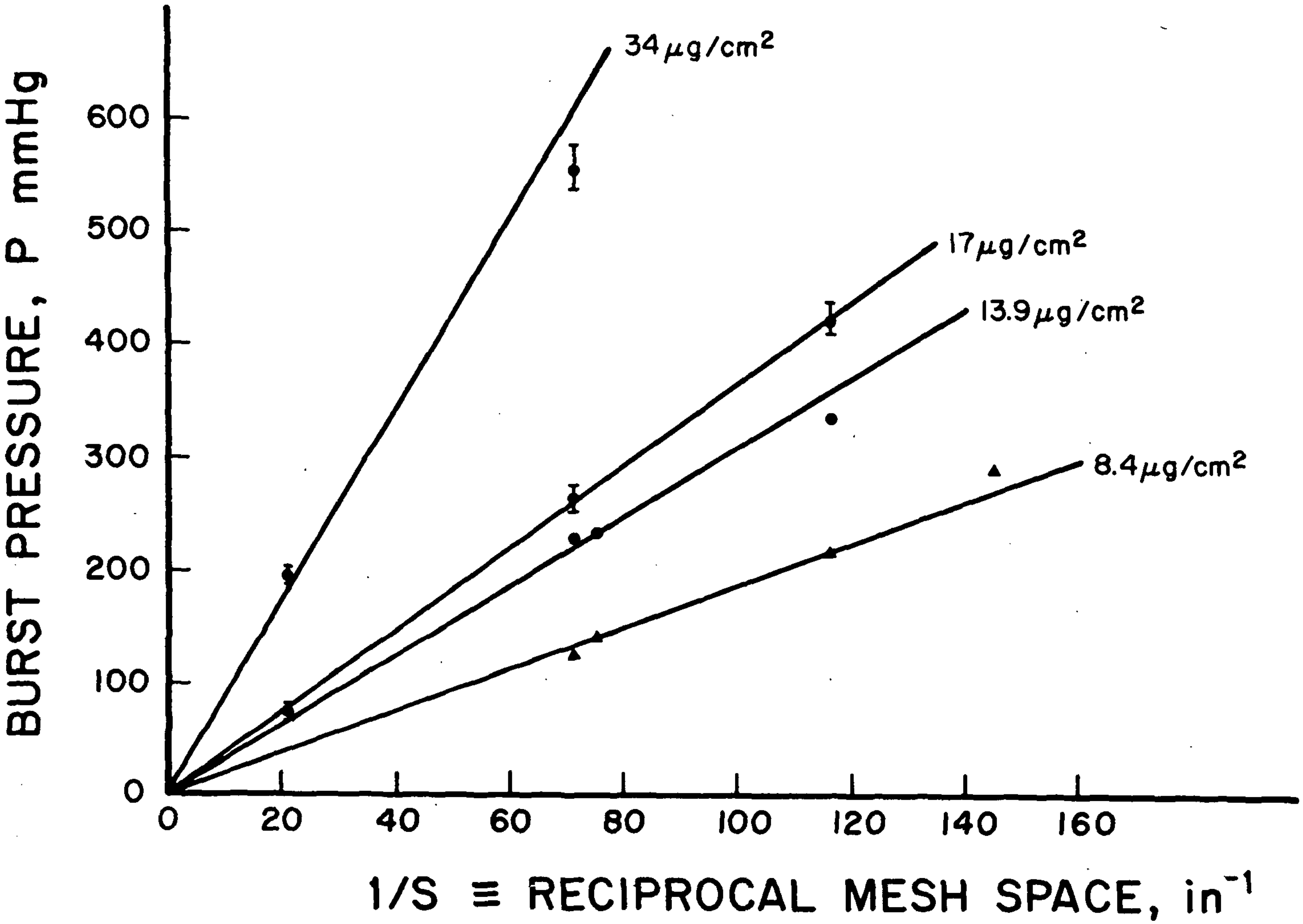

Fig. 5. VYNS pressure tests.

V. Effects of UV Exposure on Thin Films

A polymer molecule that has absorbed a UV photon may de-excite by

a) undergoing irreversible chemical change

b) emitting fluorescent radiation

c) distributing its energy among several neighboring chemical bonds (ultimately leading to heating).

Process (a) generally results in progressive deterioration of the mechanical properties of polymers, and consequently UV testing of thin film samples was undertaken in an attempt to evaluate this effect.

A. Procedure

Film samples were irradiated on test rings in a modified burst pressure apparatus. The latter was mounted inside a large vacuum chamber in such a way that it could be evacuated, sealed off, and pressurized without breaking vacuum in the large tank. It was thus not necessary to disturb the samples in any way in the interval between irradiation and burst testing.

The UV source was a water-cooled hydrogen capillary discharge source equipped with a lithium fluoride window. Intensity of the ultraviolet radiation was monitored by a gold photodiode placed adjacent to the sample. The calibration of the diode is approximate and probably good only to within a factor of 2. After exposure, film samples were allowed to cool for approximately 10 minutes prior to burst testing.

B. Results

During the course of the tests, samples were subjected to integrated exposures ranging from approximately 20 to 400 minutes solar equivalent at residual chamber pressures ranging from 0.09 to 5×10^{-6} Torr.

Reductions in burst pressure showed little or no correlation with exposure time as may be seen from the data listed in Table I for Parylene N. Data for other materials tested, although not as extensive, suggest similar behavior.

All materials with the exception of VYNS were, however, affected by the presence of residual air in the chamber during exposure as may be seen from Table II.

C. Discussion

The absence of any noticeable effects of UV exposure on VYNS films is striking. It must be pointed out, however, that the thickness of the VYNS samples was approximately two and a half times that of the others. Also notable is the apparent lack of correlation between burst pressure degradation and exposure time, suggesting that after the occurrence of initial damage, further degradation is inhibited.

Since the absorption coefficients of polymers in the X- and vacuum UV regions are extremely large, it is reasonable to suppose that the radiation affects only a surface layer whose depth increases very slowly. If this is so, it may partially explain the apparent resistance of VYNS since the surface layer in that case presumably represented a much smaller fraction of the total film thickness than in the case of the other samples. This proposition could easily be checked by repetition of some of the measurements on samples of different thicknesses.

Table I. Percent reduction in burst pressure for 10 μg/cm^2 Parylene N samples exposed at 0.09 Torr residual pressure

Exposure (min)	Reduction (%)
18	57
55	53
145	60
290	80
325	78
380	73

Table II. Reduction in burst pressure for several residual pressures. Exposures ranged typically from 100 to 300 minutes. The number in parentheses following each entry indicates the number of separate measurements from which the value is derived.

Material	Thickness, μg/cm^2	Reduction in stated pressure (Torr), %			
		0.09	4×10^{-3}	10^{-4}	5×10^{-6}
VYNS	24	0 (3)	-	-	-
Formvar	10	37 (2)	-	26 (3)	28 (4)
Parylene C	12.9	10 (2)	65 (1)	0 (1)	0 (3)
Parylene N	10	67 (6)	13 (1)	29 (1)	21 (3)